Chapter 26
Investigating the Mechanical Properties and Pitting Potential of Heat-Treated AISI 4340 Steel in Various Corrosive Environments

Shailendra Singh Bhadauria, Varun Sharma, and Ajay Gupta

Abstract The corrosion and electrochemical behavior of high-strength steel AISI 4340 with or without nitrocarburizing heat-treated conditions was studied using salt spray test under 5% NaCl for 24 hours. Electrochemical experiments were also carried out under corrosive environment of a 1N H_2SO_4. Without heat-treated results obtained by electrochemical test between potential and *log* of ampere, it yields the value of corrosion potential to 269.2 mV, and in case of heat-treated sample, value obtained is to be -431.918 mV. For heat-treated samples, the rate of corrosion (I_{corr}) shows a continuous shifting of graph toward a positive direction, whereas in case of without heat-treated sample, the rate of corrosion (I_{corr}) for HT sample is higher. In salt spray test, the more corrosion product was found to be deposited on surface of heat-treated specimen. Surface morphology of the salt spray specimen is observed under SEM and optical microscope. It reveals large numbers of corrosion pits, with heavily corroded surface. It was caused due to the decrement of the chromium content in high-strength steel with an increase of nitrocarburizing heat treatment temperature. It was observed that with an increase in heat treatment time, Vickers hardness values of 4340 steel increases from 310.8 to 468.2 HV due to increase of nitrogen (N) content over the compound layer.

Keywords Ultra-high-strength steel · Corrosion rate · Electrochemical behavior

26.1 Introduction

The use of high-strength steel increases day by day in various engineering fields. High-strength steel components operating in various corrosive environments require an engineering approach grounded in the precise understanding of corrosion failure High-strength steels contribute 7–20% of commercial and military aircraft weight, and such components can be exposed to the various corrosive environments.

S. S. Bhadauria (✉) · V. Sharma · A. Gupta
Department of Industrial and Production Engineering, Dr B R Ambedkar National Institute of Technology Jalandhar, Jalandhar 144011, India
e-mail: bhadauriass@nitj.ac.in

In order to achieve high-strength-to-weight ratio, the manufacturers are adopting various heat treatment methods, which simultaneously increase the corrosion problems [1]. The high-strength steel AISI 4340 is a medium carbon steel, and nitrocarburizing heat treatment is the best-suited heat treatment to achieve high mechanical properties with corrosion and wear properties [2]. Liquid nitrocarburizing is a thermochemical diffusion process of nitrogen and carbon atoms into the specimen surface [1]. During liquid nitrocarburizing heat treatment, the surface of the high-strength steel gets enriched with a high amount of nitrogen atoms present at the compound layer after heat treatment which is also referred as white layer [3]. The small amount of carbon during heat treatment is also deposited over the compound layer, as reported earlier [4, 5]. After heat treatment, the steel surface consists of two different phase's compound layer present over the surface of the steel and diffusion zone underlying to compound layer. The main constituents of the compound layer are ε-Fe_{2-3}(C, N) and γ'-Fe_4(C, N), which is responsible for the improvement in wear and corrosion resistance properties. The depth and concentration of the ε-Fe_{2-3}(C, N) and γ'-Fe_4(C, N) phase present over the compound layer are dependent on the time and temperature of the heat treatment [6, 7], while the diffusion zone improves fatigue strength when compared to an untreated material. In this zone, N and C atoms are dissolved interstitially in the ferrite lattice and form nitride precipitates [11], and with the increase of heat treatment time, the concentration of N and C atoms increases which increase the fatigue strength of the heat-treated sample. However, it was found that in other heat treatment methods, which are similar to liquid nitrocarburizing such as plasma nitriding and ion nitriding decrease the chromium content with the increase of heat treatment temperature. C. X. Li and T. Bell reported earlier that the heat treatment temperature above 500 °C reduces the chromium content in the steel substrate [8]. The same effect was also reported earlier by Xi [9]. The chromium content is responsible for high corrosion resistance properties of the stainless steel, which contains more than 10% of chromium content which shows a high corrosion resistance properties compared to steel 300M and Aermet100 in salt spray test [10].

Various heat treatment processes are already in use for improvement of mechanical and corrosion resistance properties, the use of liquid nitrocarburizing heat treatment for high-strength steel at high temperature needs to be studied for further understanding of behavior of AISI 4340 in terms of mechanical and corrosion resistance properties with the increase of heat treatment time at 570 °C temperature. A liquid nitrocarburizing is a low-cost heat treatment technique, but instead of focusing toward lower-cost heat treatment techniques, it is desired to determine the effect of this heat treatment over high-strength steel AISI 4340, and that is why in this work, hardness samples heat-treated for 1, 2, 4 and 6 h were used to study the effect of compound layer on hardness value of the sample treated for different hours, and one sample for both salt spray test and electrochemical test were heated for 4 hours and then tested in NaCl and 1N H_2SO_4 for determination of corrosion properties of AISI 4340.

26.2 Experiment

26.2.1 Experimental Material and Heat Treatment

The steel used in this investigation was AISI 4340. The chemical composition is given in Table 26.1.

The material was received in the form of 30 mm diameter bars. A bar is cut into nine pieces to make two samples of size 10 mm diameter and 25.4 mm long round bar for electrochemical test, and 7 samples of size full ring with a 10 mm thickness out of which two samples were used for salt spray test and remaining 5 used for the micro-hardness test as shown in Table 26.2. All the specimens were grounded to a surface finish of 0.39 μm. For the comparative analysis of nitrocarburizing heat treatment on pitting corrosion potential and corrosion rate, one of the electrochemical test samples and salt spray specimen were heat treated for 4 hours at 570 °C, and four hardness samples were heat treated to determine the effective heat treatment hours 1, 2, 4, and 6 h on hardness value. In heat treatment processes, the specimens are dipped in a salt bath container which is continuously heated via electric furnace which maintains a temperature of 570 °C, and the specimens were removed after 1, 2, 4, and 6 h as shown in Table 26.3 and instantly quenched into water afterward kept in room for 1 hour; after heat treatment, both with and without heat-treated specimens were used for electrochemical test, salt spray test, and micro-hardness test.

26.2.2 Salt Spray Test

The corrosion rate of both with and without heat-treated ultra-high-strength steel specimens was evaluated by using the salt spray test; the test was conducted according to ASTM B-117 standard for 24 hours in the test environment of 5% NaCl having a pH value of 6.8. The test chamber maintains a temperature of 35 ± 2 °C, which was used to simulate the corrosive environment. All the materials were weighed before and after removing corrosion products. The mass increment and loss were calculated to determine the corrosion rate using Eq. 26.1.

$$\text{Corrosion Rate (mpy)} = \frac{\text{Sample Weight Loss (g)} \times 5.34 \times 105}{\text{Sample Density}\left(\frac{\text{g}}{\text{cm}^3}\right) \times \text{Sample Area}\left(\text{in}^2\right) \times \text{Time Exposure (h)}}$$

$$(26.1)$$

Table 26.1 Chemical composition of AISI 4340

Steel	C	Si	Mn	P	S	Cr	Mo	Ni	Al
AISI 4340	0.414	0.250	0.660	0.030	0.009	1.200	0.311	1.379	0.002

Table 26.2 Sample size

Experiment	Sample size	No. of sample
Electrochemical test	Dia. 10 mm, Hg. 20 mm	2
Salt spray test	Dia. 64 mm, Hg. 10 mm	2
Hardness test	Dia. 30 mm, Hg. 10 mm	5

Table 26.3 Nitrocarburizing heat treatment condition

No. of sample	Heat treatment temperature (°C)	Heat treatment hours
1	570	1
1	570	2
3	570	4
1	570	6

26.2.3 Potentiodynamic Polarization Test

The electrochemical corrosion of the high-strength steel AISI 4340 was evaluated through potentiodynamic polarization tests using Model: G750, Make Gamry Instruments; samples were taken from the billet of AISI 4340 to make specimens of 10 mm diameter × 25.4 mm long round bar. The corrosion behavior of the samples was examined in a 1N H_2SO_4 solution prepared using 0.5 mol of H_2SO_4 in 1 L of the solution, and then H_2SO_4 was added slowly in 900 ml water to make a solution of total 1 L. The tests were carried out using platinum as the counter electrode and the test specimens as the working electrode. A scan rate of 0.6 V per hour for both with or without heat-treated specimens was used.

The specimen was immersed in the solution to make its open-circuit potential (E_{ocp}) become stabilized, and then the potentiodynamic polarization was performed. Potentiodynamic polarization curves were obtained by changing the electrode potential as listed in Table 26.4 with a scan rate of 0.6 V per hour.

26.2.4 Hardness Test

A hardness test performed on total five specimens in which four of them were heat treated for 1, 2, 4 and 6 hours. To investigate the effect of compound layer deposited due to different heat treatment time, hardness test was performed at 10 kg load and 10 seconds dwell time. A diamond indenter was used as indenter, the impression of the intender was recorded by measuring the diagonals of the indent impression.

Table 26.4 Test conditions under which potentiodynamic polarization test was performed

S. No.	Parameters	With HT 4 hours	Without HT
1	Specimen area	1.76 cm^2	1.76 cm^2
2	Test solution	1N H_2SO_4	1N H_2SO_4
3	Electrode	Cathode: Platinum electrode	Cathode: Platinum electrode
4	Open-circuit potential	Min: -400 mV, Max: 334.7 mV	Min: 299.7 mV, Max: 1.585 V
5	Current	Min: 21.87 μA, Max: 228.4 mA	Min: 455.5 pA, Max: 2.070 μA
6	Scan rate	0.6 V/h	0.6 V/h

26.3 Result and Discussion

26.3.1 Salt Spray Test

In salt spray test, bolt HT and WHT sample were kept into the salt spray chamber for 24 hours. The corrosion rates of AISI 4340 in both HT and WHT conditions are given in Table 26.5. It can be seen from Fig. 26.1 that AISI 4340 with nitrocarburizing heat treatment has a large amount of red rust deposited over the surface of the specimen as the weight loss is 0.20 g and without heat-treated sample shows less amount of red rust and its weight loss is 0.15 g.

$$\text{Corrosion Rate (mpy)} = \frac{\text{Sample Weight Loss (g)} \times 5.34 \times 105}{\text{Sample Density}\left(\frac{g}{cm^3}\right) \times \text{Sample Area}\left(in^2\right) \times \text{Time Exposure (h)}}$$

where the density of high-strength alloy steel AISI 4340 is 7.85 g/cm^3.

   Time exposure is 24 h.
   Sample area is 5.30 in^2.

Table 26.5 Weight loss calculated from salt spray test for WHT and HT sample

Specimen condition	Weight loss (g) after 24 h time exposure	Corrosion rate (mpy)
AISI 4340 WHT	0.15	80.21
AISI 4340 HT	0.20	106.95

Fig. 26.1 Salt spray tested specimen in 5% NaCl after 24 h in spray chamber WHT specimen on left and HT specimen on the right

26.3.2   Open-Circuit Potential (OCP)

One simple way to study the film formation and passivation of implants/alloys in a solution is to monitor the open-circuit electrode potential as a function of time. A rise of potential in the positive direction indicates the formation of a passive film, and a steady potential indicates that the film remains intact and protective.

An open-circuit potential as a function of time for two materials tested in the present investigation is given in Figs. 26.2 and 26.3. It is clear that both the tested materials, i.e., AISI 4340 HT and WHT in 1N H_2SO_4 solution, are showing a continuous shifting toward more positive values with time which clearly indicates that the
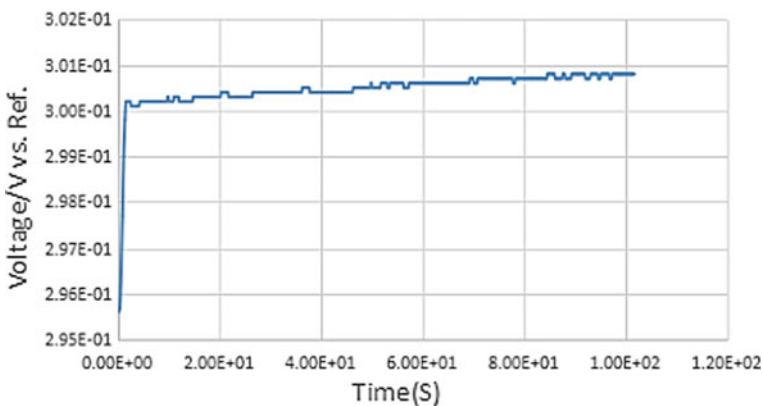
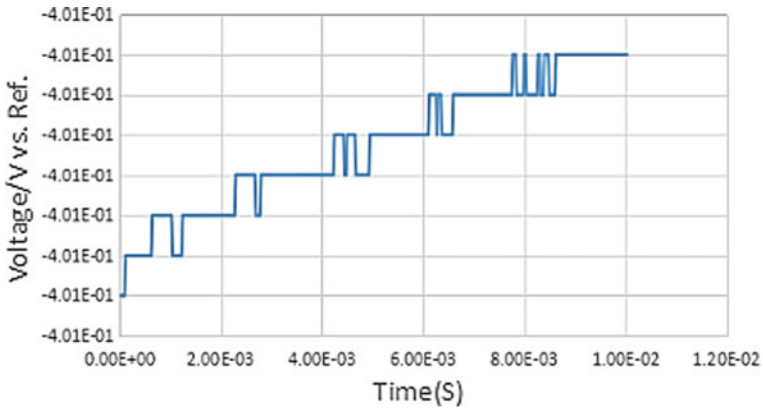**Fig. 26.2** Open-circuit potential as a function of time for WHT AISI 4340 in H_2SO_4 solution at 35 °C

Fig. 26.3 Open-circuit potential as a function of time for HT AISI 4340 in 1N H_2SO_4 solution at 35 °C

formation of a passivation layer on their surfaces. Further, more shift in the positive direction for WHT AISI 4340 steel has observed. The continuous formation and breakage of film formation are observed in HT specimen which is a low amount of chromium content in the HT specimen.

26.3.3　Potentiodynamic Polarization Study

Figure 26.4 shows the typical polarization curves of AISI 4340 for HT and WHT steel specimen in 1N H_2SO_4 solution. It is obvious that the WHT AISI 4340 has the
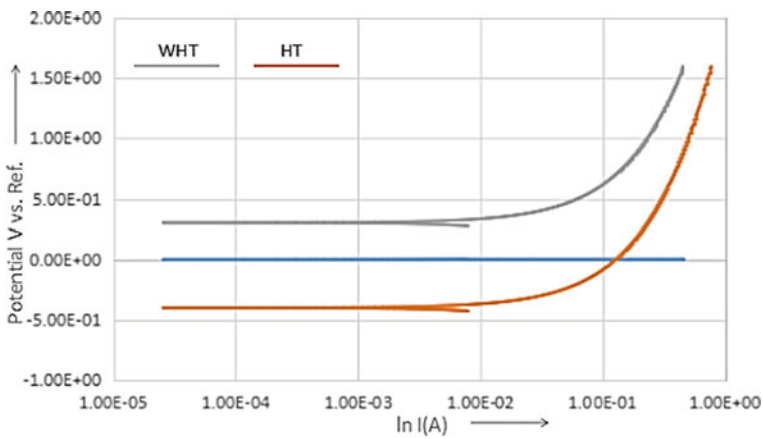

Fig. 26.4 Polarization curve for HT and WHT AISI 4340 specimen in 1N H_2SO_4 solution at 35 °C

most positive open-circuit potential value higher than HT AISI 4340. The potential is characterized by the transition from cathodic to anodic current at the corrosion potential (E_{corr}). The value of corrosion potential and corrosion rate is obtained by plotting a graph between potential (V vs. Ref) and log of ampere (Ln A) using Tafel fit curve in EC lab software, the E_{corr} value for WHT specimen obtained from the software is 269.202 mV which is higher than −431.918 mV value of HT specimen, and the value of I_{corr} is 11.48 mA, which is higher than WHT specimen value, i.e., 0.74×10^{-4} mA. The HT specimen shows the fastest corrosion as shown in Figs. 26.5 and 26.6, and the lower and higher values of corrosion potential and corrosion rate of HT sample are due to the difference in chromium content which occurs after the heat treatment processes. It can be seen that corrosion potentials for WHT specimen are nobler because of the presence of more number of chromium atoms in the steel substrate indicating that different amount of chromium atoms present in both the
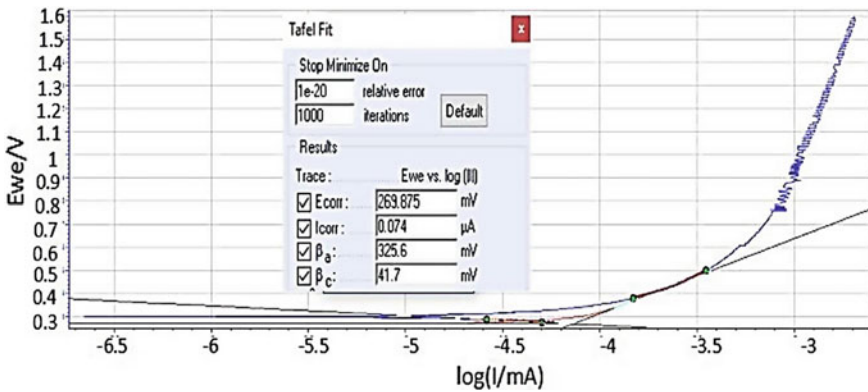

Fig. 26.5 Tafel fit curve plotted against the data obtained from electrochemical experiment for WHT sample
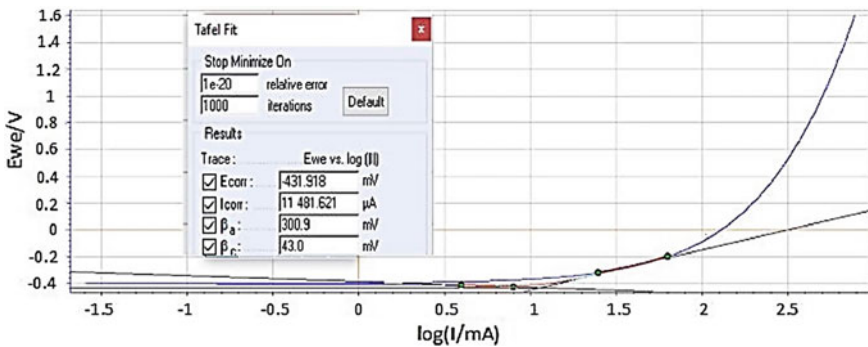

Fig. 26.6 Tafel fit curve plotted against the data obtained from electrochemical experiment for HT sample

specimens is responsible for a high amount of red rust deposition on HT sample. An SEM micrograph of nitrocarburizing heat treated for 4 h at 570 °C specimen shows a martensite microstructure with white layer deposited at the top of the specimen as reported by [10, 12–15] earlier shown in Figs. 26.7 and 26.8 (Table 26.6).

The corroded salt spray specimen was cleaned using a phosphoric acid solution to remove the corrosion product from the surface of both the specimens, the specimen was weighed before, and after removing corrosion products, the surface of both the specimens was polished using polishing cloth wheel and aged under Nital solution before performing SEM of the specimen.

The SEM image of WHT and HT specimen was shown in Figs. 26.9 and 26.10, respectively; it was clearly observed that the WHT specimen shows a less pitting effect, and the pits were uniformly distributed over the surface; on the other side HT

Fig. 26.7 SEM micrograph of nitrocarburizing heat-treated AISI 4340 specimen shows a compound white layer deposited at the surface
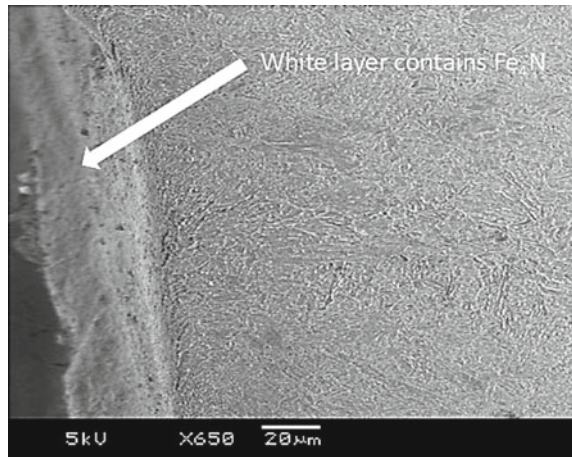
Fig. 26.8 SEM micrograph of the nitrocarburizing heat-treated sample at 570 °C for 4 h shows a martensite microstructure after heat treatment
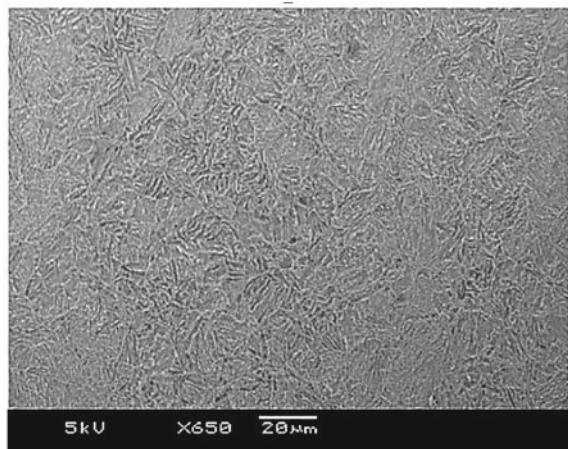
Table 26.6 Values of the parameters observed from polarization curves

Material	E_{corr}/mV versus Ref	I_{corr}/mA	bc/mV versus Ref	ba/mV versus Ref
WHT sample	269.202	0.74×10^{-4}	41.5	328.9
HT sample	−431.918	11.48	43	300.9

Note E_{corr} corrosion potential; I_{corr} corrosion current density; *ba* anodic Tafel slope; *bc* cathodic Tafel slope

Fig. 26.9 SEM image of WHT specimen at 570 °C for 4 hours shows a uniformly dispersed pitting over the surface of the specimen
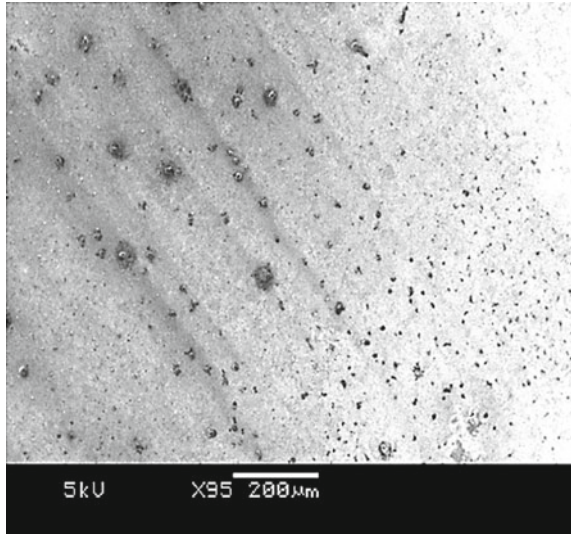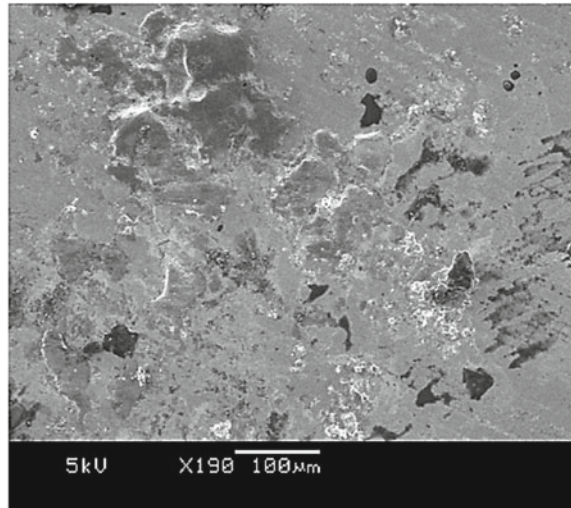

Fig. 26.10 SEM image of HT specimen shows that surface is heavily corroded after salt spray test
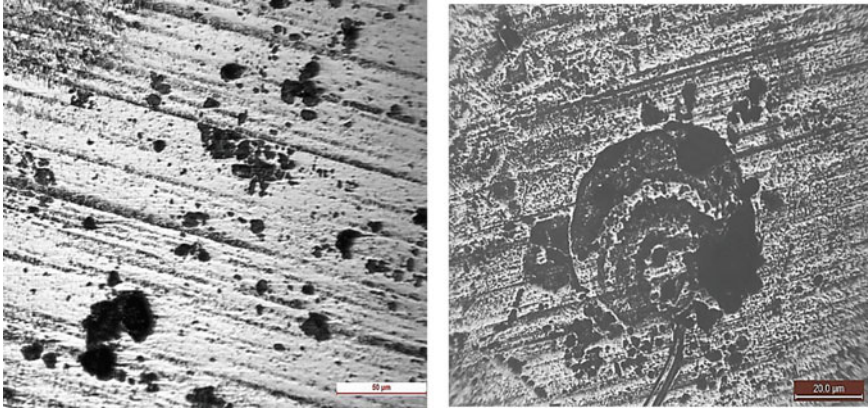
Fig. 26.11 Optical image of WHT (on left) and HT (on right) 4340 steel specimen

specimen, it has dense and large pits. Figure 26.9 shows that the WHT specimen is having less number of pits, which is due to the more chromium content in comparison with HT sample, which gets reduced after high-temperature heat treatment. The HT specimen contains martensite structure with very less or no chromium atoms which reduces corrosion resistance properties of the steel and with the addition of chromium content in steel substrate pitting corrosion resistance properties gets improved as reported earlier [10]. In support of SEM images, an optical was also performed on both HT and WHT specimens, which shows that an HT specimen is corroded heavily, and the size of pits was very large as shown in Fig. 26.11.

26.3.4   Hardness Test

Hardness values were measured on Vickers hardness tester model VM-50, at 10 kg load and 10 seconds dwell time; the observations are listed in Table 26.7 (Fig. 26.12).

With Vickers hardness test results, it was observed that with the increase of heat treatment time, the hardness value increases; for WHT specimen, the average value of five readings gives hardness value equal to 310.8 HV, and with an increase of time, the hardness value reaches to 468.2 HV for 6 hours heat treatment. The compound layer is very hard and brittle in nature, which is responsible for the increase of hardness value as moving from the inner core to the compound layer [16]. The diagonals of the diamond intender were automatically calculated by the hardness testing machine, and it was observed that the impression of the indenter is deeper in WHT specimen and impression getting shallow with the increase of heat treatment time. The N atoms are responsible for an increase of hardness of the specimen, which makes surface brittle and responsible for the shallow impression of the indenter. This shows that a gamma-phase compound layer is deposited on the heat-treated sample, and with

Table 26.7 Vickers hardness values for WHT and HT specimen

| Load and dwell time	Without HT	HT 1 hour	HT 2 hours	HT 4 hours	HT 6 hours
10 kg/10 s	304 HV a—0.2596 mm b—0.2474 mm	385 HV a—0.2192 mm b—0.2195 mm	440 HV a—0.2064 mm b—0.2044 mm	440 HV a—0.2050 mm b—0.2057 mm	477 HV a—0.1989 mm b—0.1955 m
10 kg/10 s	291 HV a—0.2527 mm b—0.2521 mm	413 HV a—0.2112 mm b—0.2126 mm	440 HV a—0.2071 mm b—0.2037 mm	470 HV a—0.1996 mm b—0.1976 mm	490 HV a—0.1928 mm b—0.1962 mm
10 kg/10 s	320 HV a—0.2425 mm b—0.2392 mm	402 HV a—0.2166 mm b—0.2132 mm	454 HV a—0.2051 mm b—0.1990 mm	472 HV a—0.2017 mm b—0.2044 mm	480 HV a—0.1976 mm b—0.1955 mm
10 kg/10 s	306 HV a—0.2473 mm b—0.2453 mm	424 HV a—0.2153 mm b—0.2030 mm	488 HV a—0.1962 mm b—0.1935 mm	442 HV a—0.2508 mm b—0.2037 mm	447 HV a—0.2051 mm b—0.2024 mm
10 kg/10 s	333 HV a—0.2344 mm b—0.2377 mm	419 HV a—0.2118 mm b—0.2091 mm	440 HV a—0.2057 mm b—0.2051 mm	453 HV a—0.2024 mm b—0.2023 mm	447 HV a—0.2043 mm b—0.2041 mm
Average value	310.8 HV a—0.2473 b—0.2443	408.6 HV a—0.2148 b—0.2114	452.4 HV a—0.2041 b—0.2011	455.4 HV a—0.2119 b—0.2027	468.2 HV a—0.1997 b—0.1987
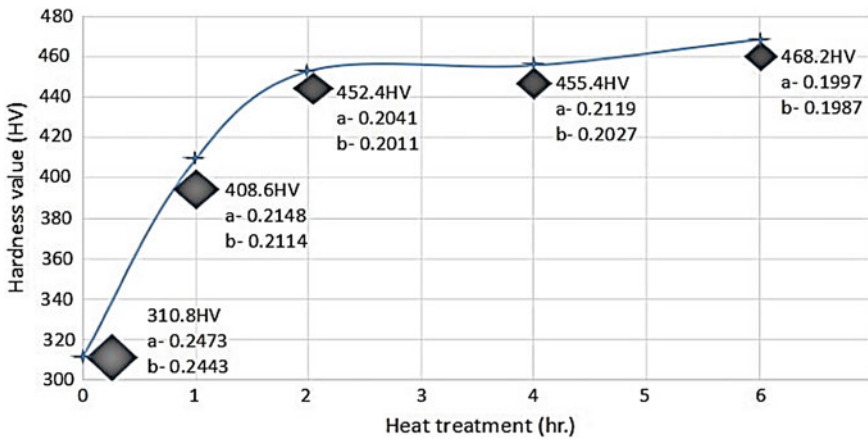
Fig. 26.12 Varitation of Vickers hardness values for different heat treatment time

the increase of heat treatment time, the concentration of N gets increased, but at the same time, chromium content gets decreased which is responsible for high corrosion rate on heat-treated sample.

26.4 Concluding Remarks

1. A liquid nitrocarburizing is a best-suited heat treatment for AISI 4340 in order to improve its wear and tear properties. It was found that with the increase of heat treatment time and temperature, nitrogen and carbon contents increase which makes the surface of the steel brittle in nature and is responsible for shallower indenter impression. This shows that hardness of the sample increases with heat treatment time.
2. Heat treatment time duration and temperature increase the Vickers hardness values, but on contrary, decrease in chromium content was observed, which reduced the corrosion resistance properties of the steel specimen.
3. A high-strength steel AISI 4340 is having a vast application in engineering fields, but it is desired to perform heat treatment, prior to its use in order to increase its application in other fields also. It was suggested for manufacture that chromium content is not getting reduced after heat treatment because it reduces the corrosion resistance properties of the steel, which may reduce the running life of the component.

References

1. Pound, B.G.: Hydrogen trapping in high-strength steels. Acta Mater. **46**(16), 5733 (1998)
2. Bhshan, B., Gupta, B.K.: Handbook of Tribology—Materials, Coatings and Surface Treatments. McGraw-Hill, New York (1991)
3. Celik, A., Karadeniz, S.: Investigation of compound layer formed during ion nitriding of AISI 4140 steel. Surf. Coat. Technol. **80**, 283–286 (1996)
4. Sun, Y., Bell, T.: Plasma surface engineering of low alloy steel. Mater. Sci. Eng. A **140**, 419–434 (1991)
5. Cho, K.S., Lee, C.O.: The effect of carbon on ion-nitriding. J. Eng. Mater. Technol. **102**, 229–233 (1980)
6. Robino, C.V., İnal, O.T.: Ion nitriding behaviour of several low alloy steels. Mater. Sci. Eng. **59**, 79–90 (1983)
7. Genel, K., Demirkol, M., Çapa, M.: Effect of ion nitriding on fatigue behaviour of AISI 4140 steel. Mater. Sci. Eng. A **279**, 207–216 (2000)
8. Li, C.X., Bell, T.: Corrosion properties of active screen plasma nitrided 316 austenitic stainless steel. Corros. Sci. **46**, 1527 (2004)
9. Xi, Y., et al.: Improvement of corrosion and wear resistances of AISI 420 martensitic stainless steel using plasma nitriding at low temperature. Surf. Coat. Technol. **202**, 2577–2583 (2008)
10. Zhong, J., Sun, M., Liu, D., Li, X., Liu, T.: Effects of chromium on the corrosion and electrochemical behaviors of ultra-high-strength steels. Int. J. Miner. Metall. Mater. **17**(3), 282 (2010)
11. Deng, X., Ju, D.: Prediction of phase composition and nitrogen concentration during the nitriding process in low-alloy steel. Mater. Res. http://doi.org/10.1590/1980-5373-MR-2015-0137
12. Sabelkin, V., Misak, H., Mall, S.: Fatigue behavior of Zn–Ni and Cd coated AISI 4340 steel with scribed damage in saltwater environment. Int. J. Fatigue 158–165 (2016)

13. Niazi, N., Nisar, S., Shah, A.: Austempering heat treatment of AISI 4340 steel and comparative analysis of various physical properties at different parameters. Int. J. Multi. Sci. Eng. **5**(10) (2014)
14. Sun, M., Zhong, P.: Stress corrosion cracking of ultra-high-strength martensite steel Cr9Ni5MoCo14 in 3.5% NaCl solution. Aerosp. Sci. Technol. 125–131 (2014)
15. Nanninga, N., Grochowsi, J., Heldt, L., Rundman, K.: Role of microstructure, composition and hardness in resisting hydrogen embrittlement of fastener grade steels. Corros. Sci. **52**, 1237–1246 (2010)
16. Figueroa, D., Robinson, M.J.: The effects of sacrificial coatings on hydrogen embrittlement and re-embrittlement of ultra-high-strength steels. Corros. Sci. **50**, 1066–1079 (2008)